Supplementary Information

Preparation of layered double hydroxide/chlorophyll *a* hybrid nano-antennae: a key step

1. Alicia E. Sommer Márquez, Facultad de Ciencias Químicas, Universidad Autónoma de Puebla, Blvd. 14 Sur, 72570 Pueblo, PUE, Mexico.

2. Dan A. Lerner*, Institut Charles Gerhardt, UMR 5253 CNRS, 8 rue Ecole Normale, 34296 Montpellier Cedex 5, France.

3. Geolar Fetter, Instituto de Investigaciones en Materiales, Universidad Nacional Autónoma de México, Circuito Exterior, C. U., 04510 México, D. F., Mexico.

4 Pedro Bosch, Instituto de Investigaciones en Materiales, Universidad Nacional Autónoma de México,
Circuito Exterior, C. U., 04510 México, D. F., Mexico.

5. Didier Tichit, Institut Charles Gerhardt, UMR 5253 CNRS, 8 rue Ecole Normale, 34296 Montpellier Cedex 5, France.

6. Eduardo Palomares, Instituto de Tecnología Química (UPV-CSIC), Universidad Politécnica de Valencia, Av. de los Naranjos, 46022 Valencia, Spain.

* Corresponding author:

Equipe Matériaux Avancés pour la Catalyse et la Santé
Institut Charles Gerhardt de Montpellier ICGM, UMR 5253 CNRS-ENSCM-UM2-UM1

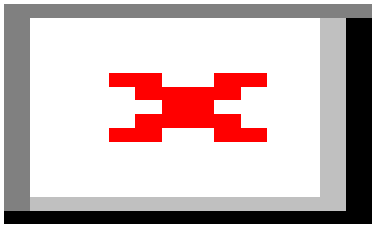

S1. Chorophyll structure, where R = CH3 (Chl *a*) or R = CHO (Chl *b*).

S2. Complements on the chromatographic separation of Chlorophyll *a* : a dismountable column for "dry" chromatography.

Classical chromatography columns possess a constriction on the upper part where the elution solvent is introduced and on the lower part where the solvent is recovered. The top one is due to the fusing together of the female ground glass joint and the column tubing. These constrictions prevent the recovery of an unbroken silica roll and adjacent molecules may end up mixed together. So a dismountable column was made with a first glass tubing in which another shorter section of glass tubing was introduced and fused to the first one to reduce the inner diameter. Then screwthreads joints (SVL) were adapted to both ends of the external tubing and fit with couplings for butt joint with a sealing ring. The inner tubing had a diameter slightly smaller than the restrictions introduced by the screwthreads joints and was used as the chromatographic column. So the silica roll obtained after elution and drying could be pushed out of the column without

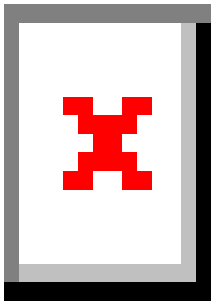

Figure S2: Appearance of the column during the separation of the crude pigments mixture. Note the separation between Chl *a* and *b*. Yellow Xantophylls are eluted first.

breaking, and revealed clear borders between adjacent spigments for an efficient recovery of Chl *a*.

The developing solvent used was a mixture of 60% n-hexane,16% petroleum ether, 10% ethyl acetate, 10% acetone and 4% methanol. Before the introduction of the pigment extract into the column, a pre-cleaning step was carried out. For the latter15 mL of n-hexane and 15 mL of distilled water were added to 15 mL of the pigment extract in acetone; the suspension was shaken a few times and left to rest for a few minutes until two layers were formed. The heaviest layer was discarded. Then, another 15 mL of distilled water were added to the supernatant phase and the same procedure was applied once more before. running the separation step.

S3. The synthesis of Mg/Al(x) and Ni/Al(x)

The M/Al(x) hydrotalcite samples were synthesized from 2.5 M water solutions of $Mg(NO_3)_2.6H_2O$, or $Ni(NO_3)_2.6H_2O$ and $Al(NO_3)_3.9H_2O$ (Merck, 99%, Aldrich 99% and 98%, respectively). A second aqueous solution, 1.86 M, was prepared with NaOH (Aldrich). The precipitation was carried out adjusting the simultaneous flow of the two solutions to maintain the pH constant at 11 in the mixture. After complete precipitation the resulting gels were treated in a microwave autoclave (MIC-I, Sistemas y Equipos de Vidrio S.A. de C.V.) operating at 2.45 GHz for 10 minutes. The microwave irradiation power was 200 W and the temperature was fixed at 80 ºC. After crystallization, the solids were recovered by decantation and washed several times with distilled water until the residual solution reached a pH value of 9. The solids recovered were dried in an oven at 60 ºC for 24 hours.

S4. X-ray diffraction of the Mg/Al(x) and Ni/Al(x)

Figure S4 displays the XRD patterns of the Mg/Al(x) and Ni/Al(x) samples. It is noteworthy that in both series of samples the intensity of the (00*l*) peaks increased and their width decreased when x, the M^{2+}/Al^{3+} molar ratio, increased. This was consistent with a regular increase of the mean crystallite coherent sizes. In Mg/Al(2) and Mg/Al(3) the (003) peaks were sharp and their position corresponds to a d_{003} basal spacing of 0.79 nm in agreement with the intercalation of nitrates as major compensating anions provided by the synthesis salts.[28]

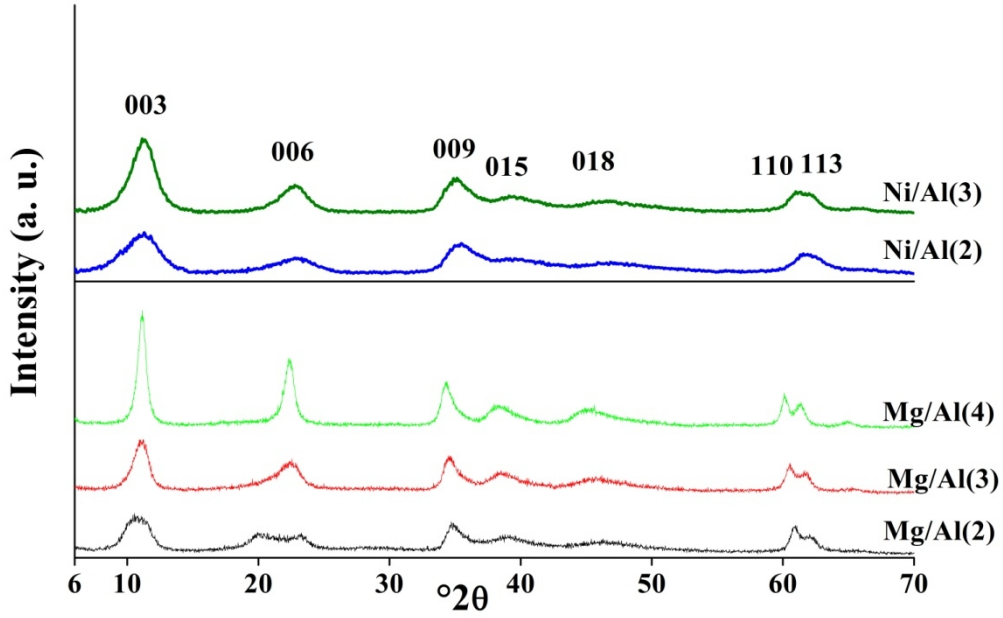

Figure S4: XRD patterns of Mg/Al(x) and Ni/Al(x) LDH

A rather different behavior was noted for Mg/Al(2) where the (003) peak were broadened suggesting a splitting which was confirmed by the two well resolved maxima observed in the harmonic (006) peak. This allowed to calculate two d_{003} basal spacings of 0.88 and 0.76 nm corresponding to the intercalation of nitrate and carbonate anions, respectively. In that sample they provided an equivalent amount of negative charges as further confirmed by chemical analysis (Table S5). In the Ni/Al(x) hydrotalcites the (00*l*) peaks appeared to be broader and less intense than in the corresponding Mg/Al(x) hydrotalcites revealing a lower crystallinity as generally observed between these two types of hydrotalcites. The d_{003} basal spacings of 0.78 nm corresponded to the intercalation of nitrate as major compensating anion.

S5 Elemental analyses

The elemental analyses (Table S5) allowed establishing the structural formula of the samples. The M^{2+}/Al^{3+} molar ratios are slightly higher than the nominal ones. NO_3^- provided by the synthesis salts and CO_3^{2-} due to the dissolution of CO_2 in water during syntheses performed in contact with air were the compensating anions. It can be noted that in the Mg/Al(x) hydrotalcites the NO_3^- content increased at the expense of the CO_3^{2-} content when the Mg/Al molar ratio increased. This suggested that the selectivity toward the monovalent anion was improved when the layer charge decreased.

Table S5. Elemental composition, suggested formula and specific surface area of the hydrotalcites.

Sample	Elemental composition (wt%)				Formula	M^{2+}/Al^{3+}	*a* (nm)	S. A. ($m^2 g^{-1}$)
	M^{II}	Al	N	C				
Mg/Al(2)	22.1	11.2	2.8	1.02	$Mg_{0.69}Al_{0.31}(OH)_2 (NO_3)_{0.15}(CO_3)_{0.06} . 0.17H_2O$	2.2	0.307	9
Mg/Al(3)	25.1	9.0	2.7	0.86	$Mg_{0.76}Al_{0.24}(OH)_2 (NO_3)_{0.14}(CO_3)_{0.05} . 0.17H_2O$	3.2	0.305	4
Mg/Al(4)	27.6	7.4	2.8	0.59	$Mg_{0.81}Al_{0.19}(OH)_2 (NO_3)_{0.14}(CO_3)_{0.03} . 0.06H_2O$	4.2	0.304	79
Ni/Al(2)	39.7	8.5	2.0	0.78	$Ni_{0.68}Al_{0.33}(OH)_2 (NO_3)_{0.15}(CO_3)_{0.07} . 0.27H_2O$	2	0.300	48
Ni/Al(3)	46.2	6.5	1.9	0.69	$Ni_{0.77}Al_{0.23}(OH)_2 (NO_3)_{0.13}(CO_3)_{0.06} . 0.06H_2O$	3.3	0.303	18

S6 Nitrogen physisorption and pore size distributions in the LDHs for Mg/Al(x) and Ni/Al(x)

All isotherms corresponded to type IV in the IUPAC classification and were characteristic of mesoporous materials (Figure 6a). According to the lower cristallinity of Ni/Al(x) than Mg/Al(x) samples previously observed by XRD, the specific surface areas of the former samples were larger than those of the corresponding latter samples. It must be underlined that these specific surface areas corresponded to the external surface area of the particles as samples were outgassed at 150 °C and nitrogen was not able to enter in the inter-lamellar space still occupied by compensating anions and water molecules. This explained the weak values obtained in the range from 4 to 79 m^2g^{-1}.

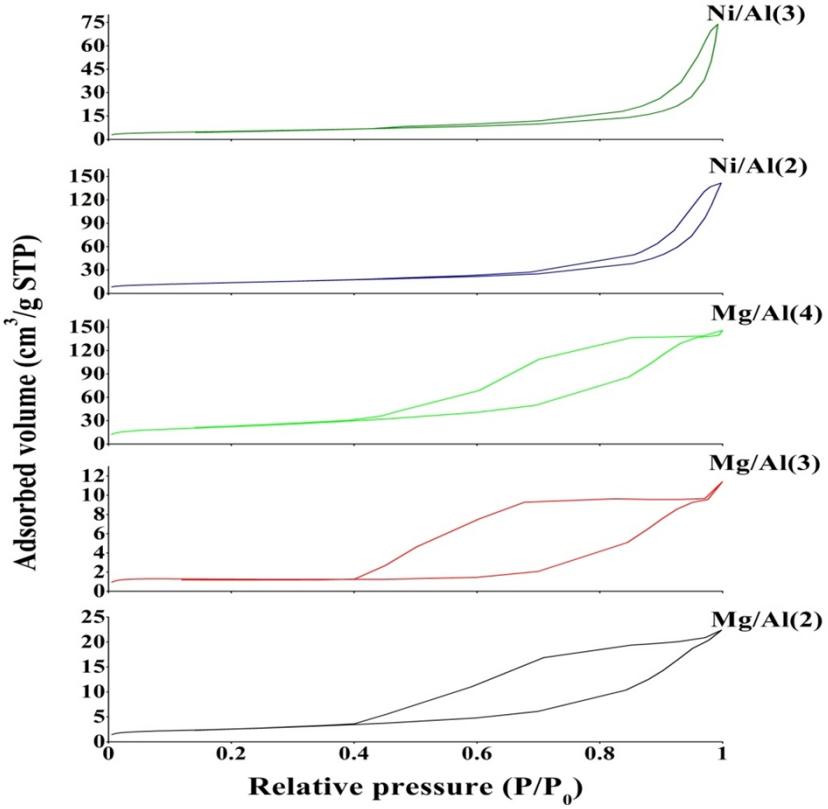

Figure 6a: Nitrogen adsorption-desorption isotherms of the different Mg/Al(x) and Ni/Al(x) hydrotalcites.

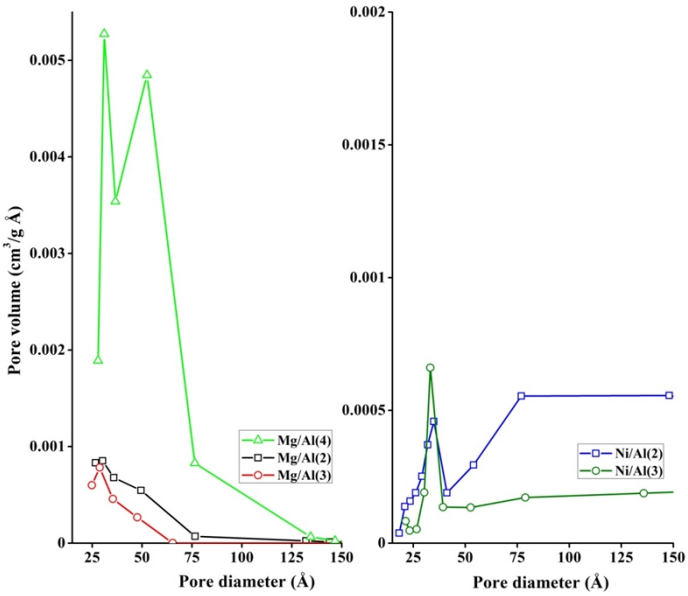

Figure S6b: Pore size distributions of the Mg/Al(x) and Ni/Al(x) hydrotalcites.

The sizes of the mesopores are in the range from 3 to 7.5 nm.

S7. Thermal analysis

The TG-DTG curves of the samples (Figure S7) exhibited the classical profile observed for hydrotalcites with a weight loss in two steps.[1] For the Mg/Al(x) samples the first weight loss of ~13 wt% due to the departure of weakly bonded water molecules occurred in the temperature range of 25 to 200 °C with a DTG peak at 130 °C. The second step in the TG profile was assigned to the elimination of structural water and to the decomposition of the anions. It corresponded to a loss of 27 wt% in the temperature range from 200 to 500 °C. It is noteworthy that the DTG peak shifted from 430 °C both in Mg/Al(2) and Mg/Al(3) to 380 °C in Mg/Al(4). For the Ni/Al(x) samples the first weight loss up to 200 °C was larger than for the Mg/Al(x) samples, i.e. of 17.5-20 wt%, with a DTG peak at 100 °C revealing a higher content of water more weakly bonded. The second weight loss reached 16 wt% and ended at 400 °C, i.e. 100 °C below the end of the second weight loss in the Mg/Al(x) samples. Moreover, the DTG peaks were shifted to 330 °C. The total weight losses of ~40 and 30 wt% in the Mg/Al(x) and Ni/Al(x) hydrotalcites, respectively, fit well to the theoretical ones.

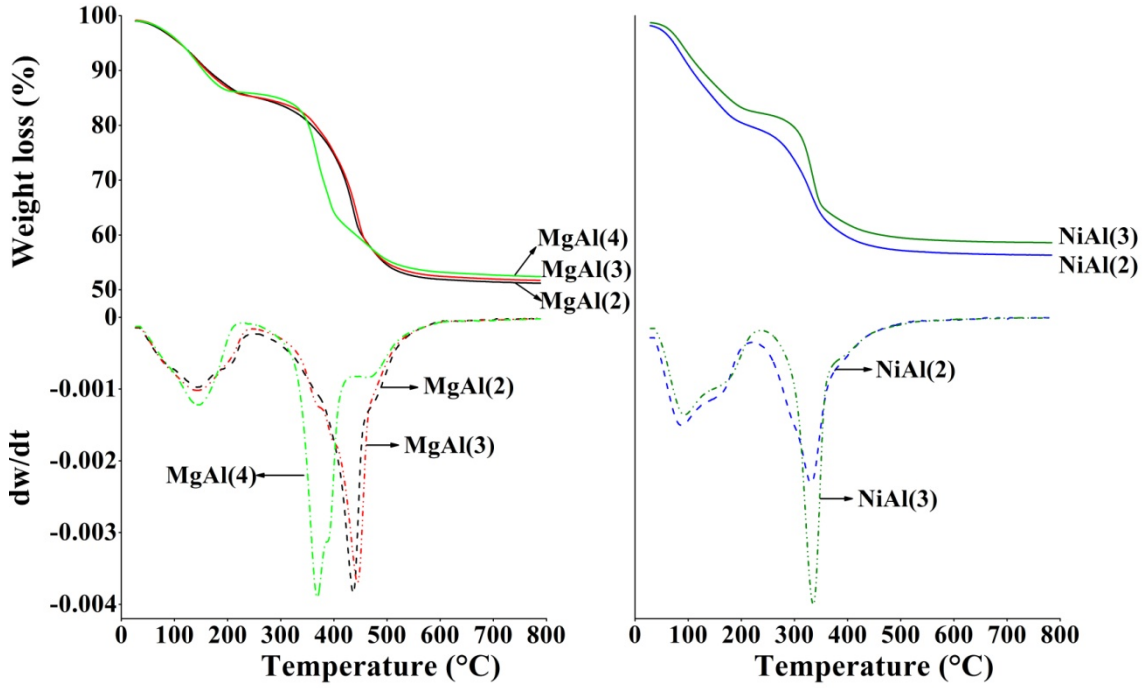

Figure S7:. Thermal analyses of the Ni/Al and Mg/Al hydrotalcites.

S8. Degradation of Chl *a* to Pheo *a* in acidic conditions

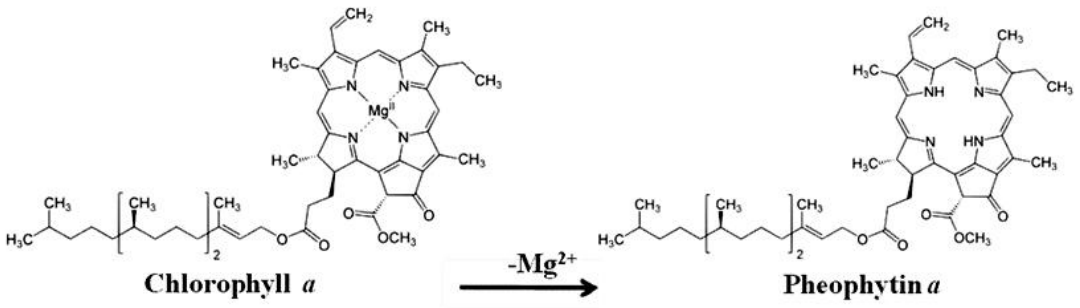

This scheme schematizes the abstraction of the Mg^{++} ion from the porphyrin ring of chlorophyll *a* to give phaeophytin *a*.

S9. Effect of the nature of the solvent used in the adsorption of Chl a on Mg/Al(x)-Chl hybrids

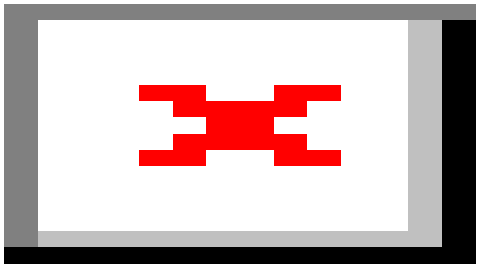

Figure S9. DRS-UV-vis (A) and fluorescence (B) spectra of Mg/Al(3)-Chl hybrids in which Chl *a* was adsorbed from acetone or diethylether.

There are no effects on the DRS-UV-vis and fluorescence spectra of the hybrids resulting from adsorption of Chl a from acetone or diethylether.

S10. Diffuse reflectance spectra of the hybrid Chl-Ni/Al(3)

The influence of the nature of the metal is clear here in the case of the Chl-Ni/Al(3) hybrid. After a few days the decomposition of Chl *a* affects most of the pigment and other products than Pheo appeared as revealed by the large broadening of the absorption bands namely in the near infra-red..

Also that effect occured irrespective of the nature of the solvent used for the adsorption of Chl a, acetone or diethyl-ether.

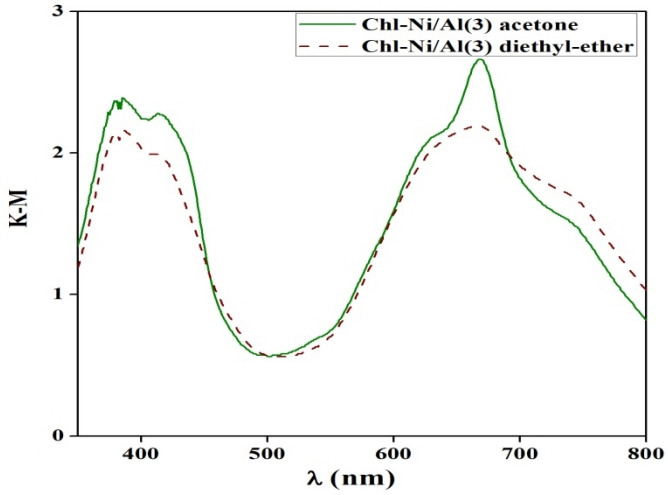

1. V. Rives, ed., *Layered Double Hydroxides: Present and Future*, Nova Science Publishers, Inc, 2001.